Dynamics of Semiconductor Lasers Subject to Delayed Optical Feedback: The Short Cavity Regime

T. Heil, I. Fischer, and W. Elsäßer
Institut für Angewandte Physik, Technische Universität, Darmstadt, Schloßgartenstraße 7, D-64289 Darmstadt, Germany

A. Gavrielides
Nonlinear Optics Center, Air Force Research Laboratory AFRL/DELO, 3550 Aberdeen Avenue SE, Kirtland AFB, New Mexico 87117-5776
(Received 15 February 2001; published 19 November 2001)

We give experimental and numerical evidence for a new dynamical regime in the operation of semiconductor lasers subject to delayed optical feedback occurring for short delay times. This short cavity regime is dominated by a striking dynamical phenomenon: regular pulse packages forming a robust low-frequency state with underlying fast, regular intensity pulsations. We demonstrate that these regular pulse packages correspond to trajectories moving on global orbits comprising several destabilized fixed points within the complicated phase space structure of this delay system.

DOI: 10.1103/PhysRevLett.87.243901 PACS numbers: 42.65.Sf, 05.45.Jn, 42.55.Px

Delayed feedback dominated systems are encountered extensively in the physical world and are of fundamental importance. They are found in models of diffusion and thermochemical reactions. In biology they occur in blood cell production, neural control, and drug delivery, and have applications in respiratory physiology [1]. Physical understanding of the dynamics of delay systems has been boosted during recent years by investigations using semiconductor lasers (SL) subject to delayed optical feedback. Basic nonlinear dynamical phenomena as period doubling [2], a quasiperiodic route to chaos [3], the Ikeda scenario [4], and bifurcation cascades [5] have already been observed in this system. In parallel, SLs are of essential importance for modern telecommunication, data transmission, and data storage technologies. There, the performance of SL systems is often degraded due to instabilities caused by even small amounts of unavoidable optical feedback from distant reflectors as, e.g., the facet of an optical fiber or a compact disc. This then requires careful isolation of the laser, thus increasing the complexity and cost of such systems. Therefore, the understanding of delayed feedback induced instabilities and its fundamental dynamical phenomena is indispensable for a wide range of practical applications. Interestingly, all the above mentioned investigations of the dynamics of SL subject to delayed optical feedback have been performed in the so-called long cavity regime (LCR) in which the external cavity length L is chosen such that the round trip frequency of the light $\nu_{\mathrm{EC}} = c/2L$ is some hundreds of MHz, and thus substantially lower than the GHz range relaxation oscillations frequency ν_{RO}. However, in many practical applications, e.g., in fiber couplers or in compact discs, the external cavity is only a few cm long. Such a reduction of L has important physical consequences. First, the ratio between the two basic system frequencies ν_{RO} and ν_{EC} is reversed. Second, the number of possible degrees of freedom is reduced. Thus, qualitatively new dynamical phenomena are to be expected for such short delay times. However, experimental investigations focusing on the nonlinear dynamical behavior of SL subject to delayed optical feedback from short external cavities are still lacking; solely stability and noise properties have been studied, e.g., see [6], and references therein.

In this paper, we present the first temporally resolved investigations of the dynamics of SLs operating in the short cavity regime (SCR). We demonstrate that this new dynamical regime is characterized by striking regular pulse packages (RPP) in the intensity dynamics of the system. Our numerical analysis demonstrates that RPP correspond to well-defined global orbits in phase space always along the same series of destabilized attractors and unstable saddle points.

Figure 1 depicts a schematic of the experimental setup. A temperature-stabilized laser diode (Sharp LT015MDO, Hitachi HLP1400) is subject to delayed optical feedback from a semitransparent dielectric mirror. The laser beam is collimated using an aspheric lens, and feedback strength is controlled with a polarizer (Pol.). The optical isolator (Iso.) shields this external cavity configuration from eventual perturbations from the detection branch. For detection, 10% (LT015MDO) and 70% (HLP1400), respectively, of the intensity in the external cavity is coupled out via the semitransparent mirror. Yet, we achieve a

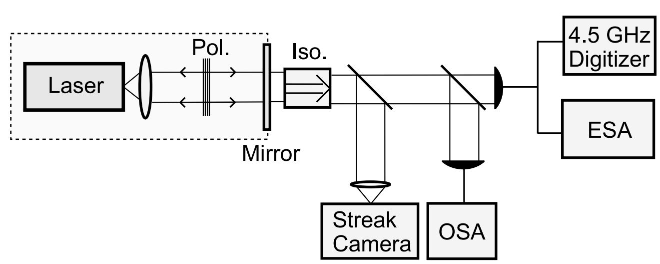

FIG. 1. Schematic of the experimental setup.

maximum threshold reduction of 11.5% and 5%, respectively. The external cavity length is varied between 1 and 7.5 cm corresponding to $2 < \nu_{EC} < 15$ GHz. We use two complimentary detection methods to record single shot measurements of the laser intensity resolving the fast round trip oscillations of the light in the external cavity. In the HLP1400 experiment, we detect the light using a single shot streak camera with an analog bandwidth larger than 50 GHz, and monitor the optical spectrum with a grating spectrometer (OSA, Anritsu MS9030A). Alternatively, in the LTO15MDO experiment, we detect the light electronically using a 8 GHz photoreceiver in combination with a Tektronix SCD5000 fast digitizer with an analog bandwidth of 4.5 GHz, and an electrical spectrum analyzer (ESA, HP 8596E). The optical spectrum is recorded with a Fabry-Perot type spectrum analyzer (OSA, Newport SR-240-C).

Figure 2 depicts a streak camera measurement of the intensity time series of the system recorded for an external cavity sufficiently short that ν_{EC} clearly exceeds the relaxation oscillation frequency ν_{RO}. Figure 2 demonstrates that the dynamics on short time scales is dominated by the delay time, whereas the long time scales are governed by the formation of a regular low frequency state: the laser intensity shows a periodic emission of regular pulse packages separated by short intervals of very low intensity. Each pulse package consists of a train of regularly spaced light pulses occurring at the round trip frequency ν_{EC}. Furthermore, the individual pulse intensities display a characteristic temporal evolution: beginning with a sudden light burst forming the first pulse of the package, the peak intensity of the individual pulses gradually decreases, until laser intensity drops to almost zero marking the time interval before the next dominant light burst. We note that this dynamics resembles the output of a mode locked laser—a series of regular pulses occurring at ν_{EC}, however, modulated by a slower envelope.

The electronic detection in the LTO15MDO experiment allows us to record longer time intervals with up to 100 RPP cycles, and provides detailed rf spectra. Figure 3a depicts a rf spectrum of this laser operating in the SCR for $\nu_{EC} \approx 4.5$ GHz and $J = 1.08 J_{th,sol}$. The inset depicts the corresponding intensity time series exhibiting very good qualitative agreement with the streak camera measurement, if one accounts for the different bandwidth. Figure 3a underlines that RPP represent a low-frequency phenomenon in the dynamics of the system: the low-frequency part of the rf spectrum consists of a dominant peak at 390 MHz corresponding to the repetition frequency of the RPP and its harmonics, whereas high frequencies are clearly dominated by the external-cavity frequency ν_{EC}. Further shortening the external cavity, we find that the RPP emission persists, and occurs over even wider parameter regimes, in particular higher injection currents. Figure 3b depicts the rf spectrum of RPP for $\nu_{EC} \approx 14$ GHz and $J = 1.80 J_{th,sol}$ displaying the dominant RPP peak and its harmonics. The RPP peak is shifted to 1195 MHz, its full width at half maximum is reduced to 3 MHz, and its peak-to-background ratio is increased to more than 30 dB. The inset of Fig. 3b depicts the corresponding time series showing the characteristic

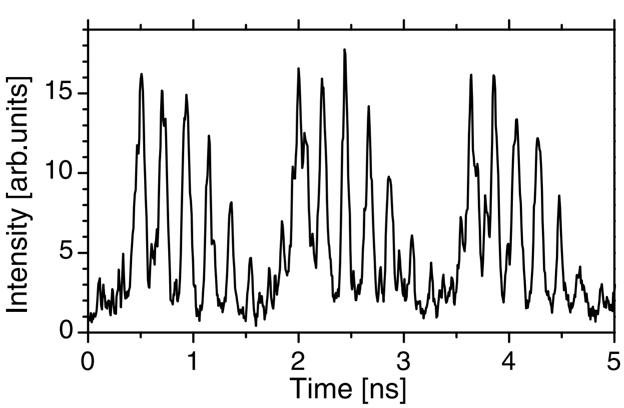

FIG. 2. Streak camera measurement of the intensity time series of the HLP1400 laser operating in the short cavity regime. The injection current is $J = 1.15 J_{th,sol}$. The external cavity is 3.2 cm long corresponding to $\nu_{EC} \approx 4.7$ GHz.

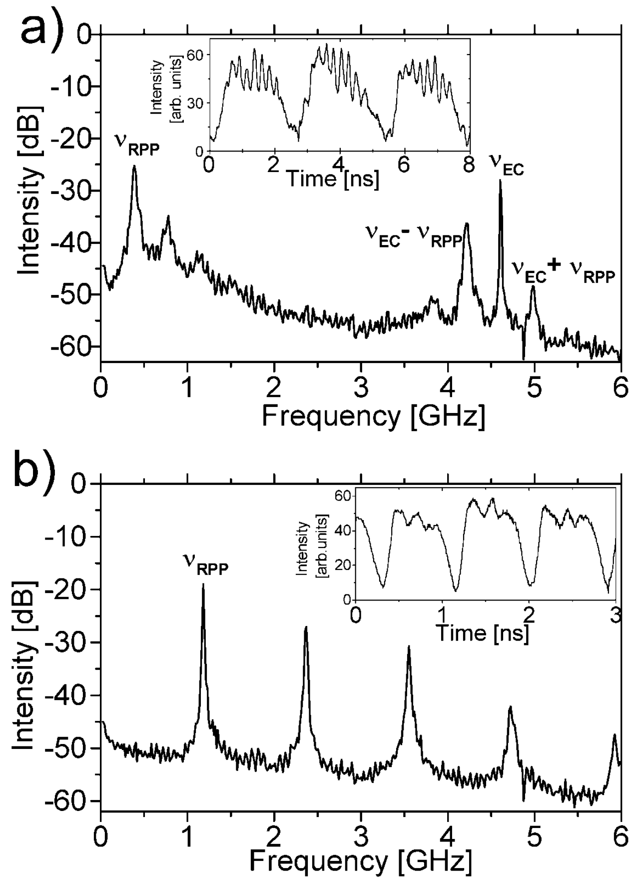

FIG. 3. Electronically detected rf spectrum and intensity time series of the LTO15MDO laser operating in the short cavity regime. (a) $J = 1.08 J_{th,sol}$ corresponding to $\nu_{RO,sol} = 1.1$ GHz, and L is 3.3 cm corresponding to $\nu_{EC} \approx 4.5$ GHz. (b) $J = 1.80 J_{th,sol}$, i.e., $\nu_{RO,sol} = 3.8$ GHz, and $L \approx 1.1$ cm, i.e., $\nu_{EC} \approx 14$ GHz.

low-frequency envelope of the RPP. The external-cavity pulsations are smeared out due to the limited bandwidth of the fast digitizer. Finally, we note, that under RPP emission, the lasers operate on several longitudinal diode modes.

We point out that RPP occur for different laser types, over wide injection current and feedback level intervals. Thus, the occurrence of RPP does not depend on a specific choice or ratio of parameters, or the use of a specific laser structure as long as the cavity is sufficiently short. These general aspects underline that the RPP indeed are the signature of a new dynamical regime. Furthermore, we find that the dynamics in this short cavity regime strongly depends on the feedback phase which is in contrast to the LCR. For the conditions in Fig. 3b, and $1.3J_{\mathrm{th,sol}} < J < 1.5J_{\mathrm{th,sol}}$ the RPP occur only over a certain phase interval, for $J = 1.08J_{\mathrm{th,sol}}$ covering approximately 0.3π rad. The phase mediates a characteristic dynamical scenario leading from stable emission to the RPP. For $J > 1.5J_{\mathrm{th,sol}}$ the RPP are present for all feedback phases but the shape of the RPP is still phase dependent. Systematic investigations are currently in progress.

We analyze the mechanisms underlying the dynamical behavior of SL in the SCR on the basis of a rate equation approach [7]. The evolution of the electric field $E(t) = A(t)\exp[i\Phi(t)]$, and of the carriers N is described by the following set of dimensionless ordinary differential equations [8]:

$$\dot{E} = (1 + i\alpha)NE + \eta e^{-i\omega\tau}E(t - \tau), \qquad (1)$$

$$T\dot{N} = P - N - (1 + 2N)|E|^2. \qquad (2)$$

In these equations, the time is normalized to the cavity photon lifetime (~1 ps) and T is the ratio of the carrier lifetime (1 ns) to the photon lifetime. The external round trip time τ is also normalized to the photon lifetime. The excess pump current P is proportional to $(J/J_{\mathrm{th,sol}} - 1)$. Finally, α is the linewidth enhancement factor, and η is the amount of feedback. A number of simplifying assumptions have indeed been made to reduce the problem to this set of equations. Multiple external cavity round trips have been ignored, as the effective feedback strength for these rapidly decreases. Only a single solitary mode and no gain saturation and cross-saturation effects are included in the calculation, even if, experimentally, the laser exhibits multimode operation. These effects are omitted here for simplicity. However, we have modeled the multimode behavior extensively, and found that the fundamental picture presented here is not altered in any significant way.

Numerical calculations indicate the following characteristics for the development of the RPP. A series of progressive merging of the destabilized external cavity modes into larger attractors precedes the appearance of the RPP. In general, very few modes are needed before RPP make their appearance. In Fig. 4 (top) we present a numerical time series of a RPP computed for values of the parameters representative of the experimental results of Fig. 3, and in particular for pumping currents well above solitary laser threshold. We have used $P = 1.15$, $T = 1710$, $\tau = 70$, $\alpha = 5.0$, and we have fixed the external cavity round trip phase $\omega\tau = -\tan^{-1}(\alpha)$ for convenience. These normalized numbers translate to a solitary relaxation frequency of 3.42 GHz, an external cavity length of 1.79 cm, and an inverse photon lifetime of $\gamma_c = 5.86 \cdot 10^{11}\ \mathrm{s}^{-1}$. The feedback rate was set at $\eta = 0.135$, close to the experimentally observed reduction of threshold relative to the solitary laser of 11%. The time series in Fig. 4 (top) has not been subjected to any filtering at the bandwidth of detection, clearly a procedure that would smear out some of the characteristic pulsations at the fast frequencies. In Fig. 4 (bottom), we show the trajectory in a projection on the plane of normalized inversion versus the phase difference $\Phi(t - \tau) - \Phi(\tau)$. The trajectory comprises three sequential cycles which are very regular, thus, ν_{EC} and ν_{RPP} appear to be very close to be commensurate. In the same plot, we have indicated the steady state solutions of the equations, nodes marked with circles and saddles by crosses. Notice also that the trajectory always visits the same external cavity modes even though they might not be sequential.

We note that dynamical features exhibiting similarities to the here reported SCR dynamics have been observed numerically in an even more simplified model [9]. This three

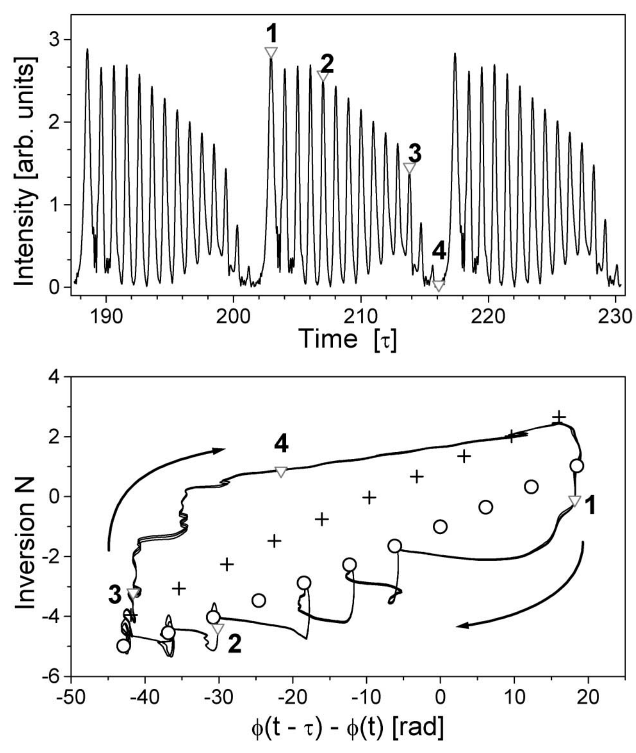

FIG. 4. Numerically computed RPP. Top: Laser intensity plotted against time normalized to τ. Bottom: RPP trajectory plotted on the normalized inversion N and phase difference $\Phi(t - \tau) - \Phi(t)$ plane. The location of the nodes is indicated by circles, and the saddles by crosses. The temporal evolution occurs clockwise; the numbers provide a one-to-one correspondence of time series and phase space portrait.

TABLE I. Classification of SL with moderate optical feedback: short cavity regime versus long cavity regime.

	Short cavity regime RPP	Long cavity regime LFF
System internal frequencies	$\nu_{EC} \gg \nu_{RO}$	$\nu_{EC} \ll \nu_{RO}$
No. of modes	Small number ~10	Large number ~100
Influence of feedback phase	Qualitative changes	No qualitative changes
Dynamics on short time scales	Regular fast pulses: $\nu = \nu_{EC}$	Irregular fast pulses: $\nu_{avg} \sim \nu_{RO}$
Dynamics on long time scales	Low-frequency phenomena: Regular global trajectory along several modes	Low-frequency phenomena: Mostly irregular (rarely regular) global trajectory along several modes

dimensional model is based on a truncation of the Fourier series expansion of the delay terms in the LK model. Accordingly, we have performed additional numerical simulations using this reduced model. The obtained agreement with the experimental results is not as good as the agreement achieved by using the full LK model underlining the importance of the delay term in the equations. Nevertheless, we underline the potential of this simplified model for future analytical investigations of the dynamics of SLs operating in the SCR.

It is very instructive for the general understanding of feedback induced instabilities in SLs to compare our SCR results to the previous investigations of the dynamics of SLs in the long cavity regime. We focus on a comparison of the short cavity RPP to the so-called low frequency fluctuations (LFF); a long cavity phenomenon which has been intensively studied during recent years [10]. Increasing the length of the external cavity, we note that the transition from RPP dynamics to LFF dynamics occurs roughly at $\nu_{RO} \gtrsim \nu_{EC}$: the short time scale dynamics becomes irregular, and dominated by relaxation oscillations. The comparison between the RPP and the LFF is condensed in Table I. We note that basic quantities as the ratio between ν_{RO} and ν_{EC}, the number of the possible degrees of freedom, and the relevance of the feedback phase are clearly different. Nevertheless, we find remarkable common features in the dynamics of RPP and LFF. In both cases, low-frequency phenomena are present which correspond to a directed global trajectory along several attractor ruins consequencing fast intensity pulsations underlying the low-frequency envelope. In the LFF, the trajectory usually backtracks irregularly, and visits different attractor ruins, whereas Fig. 4 demonstrates that in the RPP the trajectory evolves in a regular way within a well-defined looped channel along always the same series of attractor ruins. Considering the complicated phase space structure of a delay system, this is remarkable and indicates a global orbit underlying to the RPP dynamics. Interestingly, for certain parameter sets, regular states have also been observed in the LCR [11]. However, in the LCR the fast time scales are dominated by relaxation oscillations, whereas the fast time scales in the SCR are dominated by the external cavity roundtrip frequency. In conclusion, the merging of attractor ruins to a global orbit appears to be a basic phenomenon present in the dynamics of SLs subject to delayed optical feedback [12]. Because of the basic character of our experiments and numerical simulations, we conjecture that this mechanism of merging the individual attractor ruins to a large stable object may also occur in other delay systems.

A. G. gratefully acknowledges the U.S. Air Force Office of Scientific Research for support of his work; T. H. thanks EOARD for kind hospitality and financial support for his research stay at the Nonlinear Optics Center. We would like to acknowledge fruitful discussion with T. Newell and V. Kovanis at the University of New Mexico.

[1] I. R. Epstein and J. A. Pojman, *An Introduction to Nonlinear Chemical Dynamics* (Oxford University Press, New York, 1998); M. C. Mackey and L. Glass, Science **197**, 287 (1977); Longtin and Milton, Math. Biosc. **90**, 183 (1988); J. Foss, A. Longtin, B. Mensour, and J. Milton, Phys. Rev. Lett. **76**, 708 (1996); A. C. Fowler, *Mathematical Models in the Applied Sciences,* Cambridge Texts in Applied Mathematics (Cambridge University Press, Cambridge, 1997).

[2] J. Ye, H. Li, and J. G. McInerney, Phys. Rev. A **47**, 2249 (1993).

[3] J. Mørk, J. Mark, and B. Tromborg, Phys. Rev. Lett. **65**, 1999 (1990).

[4] I. Fischer, O. Hess, W. Elsäßer, and E. Göbel, Phys. Rev. Lett. **73**, 2188 (1994).

[5] A. Hohl and A. Gavrielides, Phys. Rev. Lett. **82**, 1148 (1999).

[6] K. Petermann, IEEE J. Sel. Top. Quantum Electron. **1**, 480 (1995).

[7] R. Lang and K. Kobayashi, IEEE J. Quantum Electron. **16**, 347 (1980).

[8] P. M. Alsing, V. Kovanis, A. Gavrielides, and T. Erneux, Phys. Rev. A **53**, 4429 (1996).

[9] G. Huyet, P. A. Porta, S. P. Hegarty, J. G. McInerney, and F. Holland, Opt. Commun. **180**, 339 (2000).

[10] C. Risch and C. Voumard, J. Appl. Phys. **48**, 2083 (1977); G. H. M. van Tartwijk, A. M. Levine and D. Lenstra, IEEE J. Sel. Top. Quantum Electron. **1**, 466 (1995); I. Fischer, G. H. M. van Tartwijk, A. M. Levine, W. Elsäßer, E. Göbel, and D. Lenstra, Phys. Rev. Lett. **76**, 220 (1996).

[11] A. Gavrielides, T. C. Newell, V. Kovanis, R. G. Harrison, N. Swanston, D. Yu, and W. Lu, Phys. Rev. A **60**, 1577 (1999).

[12] R. L. Davidchack, Y. C. Lai, A. Gavrielides, and V. Kovanis, Phys. Rev. E **63**, 056206 (2001).